Photothermal Agents Hot Paper

International Edition: DOI: 10.1002/anie.201506154
German Edition: DOI: 10.1002/ange.201506154

Ultrasmall Black Phosphorus Quantum Dots: Synthesis and Use as Photothermal Agents

Zhengbo Sun, Hanhan Xie, Siying Tang, Xue-Feng Yu, Zhinan Guo, Jundong Shao, Han Zhang,* Hao Huang, Huaiyu Wang, and Paul K. Chu**

Abstract: *Black phosphorus quantum dots (BPQDs) were synthesized using a liquid exfoliation method that combined probe sonication and bath sonication. With a lateral size of approximately 2.6 nm and a thickness of about 1.5 nm, the ultrasmall BPQDs exhibited an excellent NIR photothermal performance with a large extinction coefficient of 14.8 Lg^{-1} cm^{-1} at 808 nm, a photothermal conversion efficiency of 28.4 %, as well as good photostability. After PEG conjugation, the BPQDs showed enhanced stability in physiological medium, and there was no observable toxicity to different types of cells. NIR photoexcitation of the BPQDs in the presence of C6 and MCF7 cancer cells led to significant cell death, suggesting that the nanoparticles have large potential as photothermal agents.*

Owing to the superior tissue-penetration ability of near-infrared (NIR) light,[1] NIR photothermal agents have attracted considerable attention in cancer photothermal therapy (PTT),[2] drug/gene delivery,[3] and tissue engineering.[4] The ideal photothermal agent should not only have a considerable extinction coefficient and photothermal conversion efficacy in the NIR region, but also satisfy the strict safety requirements of clinical use.[5] The biocompatibility of chemical components is the first consideration to ensure safety and proper surface functionalization by means of, for example, biocompatible polymers such as PEG, which can improve the biocompatibility and facilitate tumor targeting.[6] The particle size influences both the toxicity and clearance characteristics.[7] In clinical applications, the therapy agents should be completely cleared from the human body within a reasonable period. Typically, efficient renal and liver clearance requires the agents to be smaller than 10 nm.[7c,d] Various nanoparticles with good NIR optical properties have hitherto been developed, and they exhibit efficient photothermal performance in vitro and in vivo.[2,8–21] However, very few nanoparticles meet the safety requirements, and hence, the development of new biocompatible photothermal agents is of scientific and clinical interest.

Herein, we describe the synthesis and photothermal properties of ultrasmall black phosphorus quantum dots (BPQDs), which display an excellent NIR photothermal performance and biocompatibility. Phosphorus is a vital element in the human body, amounting to approximately 660 g in an adult human and accounting for 1 % of the body weight. As one of the three allotropes of phosphorus, black phosphorus (BP), a conceptually new two-dimensional (2D) layered material, has received much interest owing to its unique layered structure and a layer-dependent bandgap of 0.3 to 2.0 eV.[22] Mechanical and liquid exfoliation methods have been adopted to prepare BP nanosheets with different numbers of layers and sizes,[23] and the products have fascinating applications in electronics and photoelectric devices.[24] However, their application in biomedicine is still in its infancy owing to the lack of suitable synthesis strategies.

We have now prepared a highly dispersed suspension of ultrasmall BPQDs with a lateral size of approximately 2.6 nm and a thickness of approximately 1.5 nm by a simple liquid exfoliation technique. As illustrated in Figure 1 a, liquid exfoliation involves ultrasound probe sonication followed by ice-bath sonication of bulk BP powder in 1-methyl-2-pyrrolidone (NMP). The ultrasmall BPQDs obtained by centrifugation were dispersed in water, and PEG was conjugated to enhance their stability in physiological medium (for more details on the synthesis, see the Supporting Information). Both probe sonication and bath sonication are commonly used in the exfoliation of 2D layered materials including BP.[23b,d] Although it seems that bath sonication is more efficient in breaking bulk BP into smaller particles than probe sonication,[23d] the use of only one of them can only result in irregular BP nanosheets (see the Supporting Information, Figure S1). In our method, probe sonication and bath sonication are combined to exfoliate bulk BP crystals into ultrasmall BPQDs. It has been reported that BPQDs can be synthesized by grinding followed by ice-bath sonication of micrometer-sized BP crystals.[23d] For comparison, probe sonication is more reproducible than grinding and commer-

[*] Dr. Z. Sun,[+] H. Xie,[+] S. Tang, Prof. X.-F. Yu, H. Huang, Prof. H. Wang
Institute of Biomedicine and Biotechnology
Shenzhen Institutes of Advanced Technology
Chinese Academy of Sciences
Shenzhen 518055 (P. R. China)
E-mail: xf.yu@siat.ac.cn

Dr. Z. Sun,[+] Z. Guo, J. Shao, Prof. H. Zhang
SZU-NUS Collaborative Innovation Center for Optoelectronic Science and Technology and Key Laboratory of Optoelectronic Devices and Systems of Ministry of Education and Guangdong Province
College of Optoelectronic Engineering, Shenzhen University
Shenzhen 518060 (P. R. China)
E-mail: hzhang@szu.edu.cn

H. Huang, Prof. P. K. Chu
Department of Physics and Materials Science
City University of Hong Kong
Tat Chee Avenue, Kowloon, Hong Kong (P. R. China)
E-mail: paul.chu@cityu.edu.hk

[+] These authors contributed equally to this work.

Supporting information for this article is available on the WWW under http://dx.doi.org/10.1002/anie.201506154.

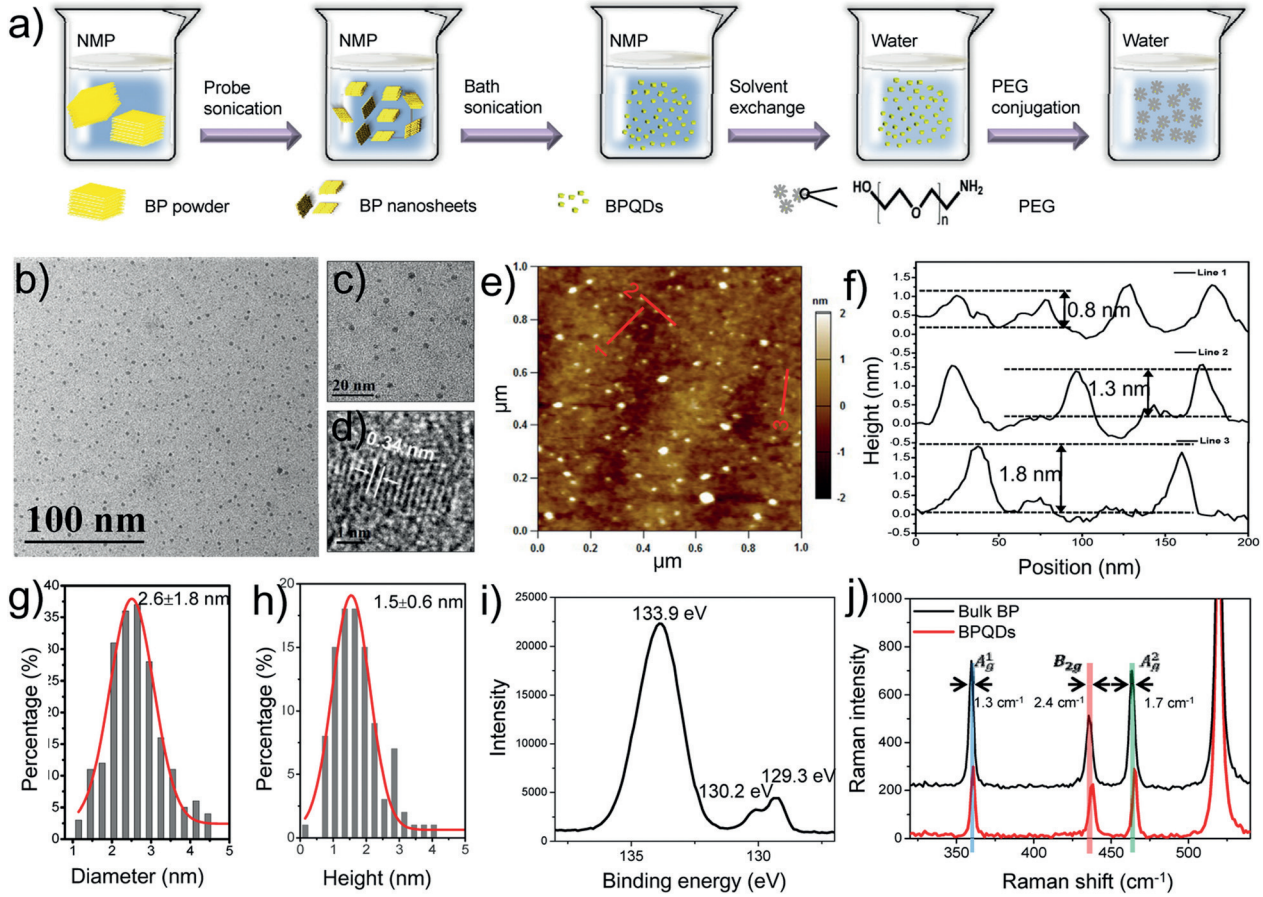

Figure 1. Synthesis and characterization of the BPQDs. a) Synthesis and surface modification. b) TEM image. c) Magnified TEM image. d) HR-TEM image. e) AFM image. f) Height profiles along the red lines in (e). g) Statistical analysis of the lateral sizes of 100 BPQDs determined by TEM. h) Statistical analysis of the heights of 100 BPQDs determined by AFM. i) XPS spectrum. j) Raman spectra.

cially available bulk BP crystals can be used directly as the starting materials in our synthesis.

Transmission electron microscopy (TEM) and atomic force microscopy (AFM) were employed to examine the morphology of the BPQDs. The TEM images in Figure 1 b and c reveal ultrasmall BPQDs, and the high-resolution TEM (HRTEM) image in Figure 1 d shows lattice fringes of 0.34 nm, which were ascribed to the (021) plane of the BP crystal.[23c] The topography of the BPQDs is shown in Figure 1 e and f, and the measured heights were 0.8, 1.3, and 1.8 nm. According to the statistical TEM and AFM analysis of 100 BPQDs (Figure 1 g, h), the average lateral size was 2.6 ± 1.8 nm and the average thickness 1.5 ± 0.6 nm, corresponding to a stack of 2 ± 1 quintuple layers (QLs) of BP. The chemical composition of the BPQDs was determined by X-ray photoelectron spectroscopy (XPS) after the sample had been sputtered for 5 min to remove any surface contaminants (see Figure 1 i and Figure S2). The BPQDs show the $2p^{3/2}$ and $2p^{1/2}$ doublets at 129.3 and 130.2 eV, respectively, which are characteristic of crystalline BP.[23b–d] Furthermore, strong sub-bands corresponding to oxidized phosphorus (i.e., PO_x) are apparent at 133.9 eV, which have been observed in previous measurements.[23b] BP is sensitive to water and oxygen and can be oxidized under visible-light irradiation. Oxidation is thus unavoidable in biomedical applications. In our study, the BPQDs were exfoliated under ambient conditions and dispersed in an aqueous solution. Hence, some surface oxidation is expected to occur. Although oxidization may influence the electrical properties of the BP nanosheets, our experiments showed that surface oxidization did not lead to a decrease in NIR absorption or a deterioration of the photothermal performance of the BPQDs.

The BPQDs were also characterized by Raman spectroscopy. As shown in Figure 1 j, the three prominent peaks can be attributed to one out-of-plane phonon mode (A_g^1) at 359.5 cm^{-1} as well as two in-plane modes, B_{2g} and A_g^2, at 436.0 and 463.3 cm^{-1}, respectively. Compared to bulk BP, the A_g^1, B_{2g}, and A_g^2 modes of the BPQDs are red-shifted by approximately 1.3, 2.4, and 1.7 cm^{-1}, respectively. A similar red shift has been observed for BP nanosheets with a few layers.[25]

The stability of the BPQDs in physiological medium is enhanced by surface modification with PEG. Although bare BPQDs are soluble in water, they aggregate in the presence of salts (Figure 2 a and Figure S3). Positively charged PEG–NH_2 (see Figure 1 a) was thus used to coat the surface of the

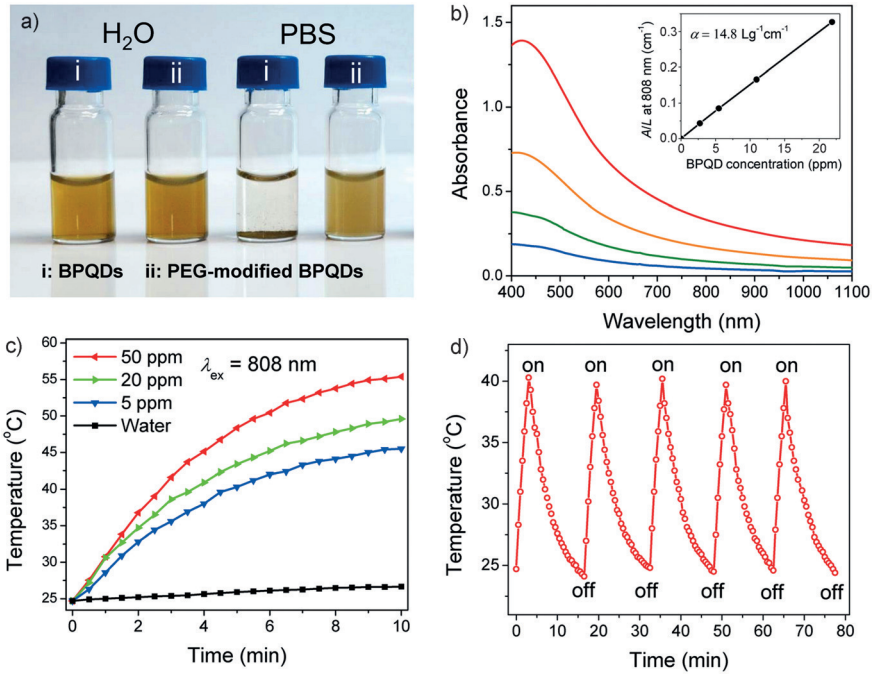

Figure 2. NIR optical properties of the BPQDs. a) Photographs of BPQDs (i) and PEG-modified BPQDs (ii) dispersed in water or PBS solution. b) Absorbance spectra of PEG-modified BPQDs dispersed in water at different concentrations. The top curve corresponds to a BPQD concentration of 22.0 ppm. For each subsequent curve, the suspension was diluted by a factor of 2. Inset: Normalized absorbance intensity divided by the characteristic length of the cell (A/L) at different concentrations for $\lambda = 808$ nm. c) Photothermal heating curves of pure water and PEG-modified BPQDs dispersed in water at different concentrations under irradiation with an 808 nm laser (1.0 W cm^{-2}). d) Heating of a suspension of the PEG-modified BPQDs in water for five laser on/off cycles.

BPQDs by electrostatic adsorption.[26] After surface modification, the zeta potential of the BPQDs changed from −26.0 to −13.2 mV. The PEG-modified BPQDs exhibited enhanced stability in physiological solutions, such as phosphate buffered saline (PBS) and cell-culture media.

The NIR extinction and photothermal properties of PEG-modified BPQDs dispersed in water solution are shown in Figure 2b. The optical absorption spectra acquired with the BPQDs show a broad absorption band spanning the UV and NIR regions and are similar to those of other 2D layered materials, such as graphene oxide (GO)[11] and WS_2.[6a] The normalized absorption intensity over the characteristic length of the cell (A/L) at $\lambda = 808$ nm at different concentrations (C) was determined (see Figure 2c), and the amount of BPQDs was determined by inductively coupled plasma atomic emission spectroscopy (ICP-AES). In agreement with the Lambert–Beer law ($A/L = \alpha C$, where α is the extinction coefficient), a linear trend was observed for the dependence of A/L on the concentration, and the extinction coefficient at 808 nm was estimated to be 14.8 Lg^{-1} cm^{-1}. For comparison, the extinction coefficient of Au nanorods (AuNRs), a common photothermal agent, was determined by the same procedures (see Figure S4). The extinction coefficient of the BPQDs (14.8 Lg^{-1} cm^{-1}) is approximately 3.8 times larger that that of the AuNRs (3.9 Lg^{-1} cm^{-1}). Compared with previously reported 2D layered materials, the extinction coefficient of the BPQDs was higher than that of GO nanosheets (3.6 Lg^{-1} cm^{-1}),[11] but lower than that of WS_2 nanosheets (23.8 Lg^{-1} cm^{-1}).[6a] Nevertheless, the use of BPQDs as ultrasmall photothermal agents is attractive.

To evaluate the photothermal properties of the BPQDs, different amounts of the PEG-modified BPQDs were dispersed in aqueous solutions and exposed to an 808 nm NIR laser (power density: 1.0 W cm^{-2}). The solution temperature was then monitored as a function of time (see Figure 2c). At a very low BPQD concentration (50 ppm), the solution temperature had increased by 31.5 °C after irradiation for 10 min. In contrast, the temperature of pure water had increased by only 2.1 °C, indicating that the BPQDs can rapidly and efficiently convert NIR light into thermal energy. Furthermore, by means of a reported method,[27] the photothermal conversion efficiency of the BPQDs was determined to be approximately 28.4 %, which is significantly higher than those of commercial Au nanoshells (13 %) and AuNRs (21 %).[13,28] A direct comparison of the photothermal performance of the BPQDs and AuNRs is shown in Figure S5. Solutions containing 20.3 ppm BPQDs or 77.9 ppm AuNRs were prepared to account for their optical densities at 808 nm. After the same 808 nm laser irradiation, a larger temperature increase was observed for the BPQD solution. Considering that smaller amounts of the BPQDs were used, the photothermal performance of the BPQDs is clearly superior to that of the AuNRs.

To further assess the photothermal stability of the BPQDs, the temperature of a PEG-BPQD dispersion upon radiation with an NIR laser for 5 min (laser on) was monitored with time, followed by natural cooling to room temperature after the NIR laser has been turned off (laser off). This cycle was repeated five times to evaluate the photostability of the BPQDs. The photothermal effect of the BPQDs did not deteriorate during temperature elevation, highlighting their large potential as photothermal agents.

Nanomaterials used in biomedicine must be of sufficient biocompatibility, and therefore, the cytotoxicity of the BPQDs to several types of cells was examined (Figure 3). The standard methyl thiazolyl tetrazolium (MTT) assay was carried out to determine the relative viabilities of HSC (hepatic stellate cells), 293T (human embryo kidney cells), C6 (glioma cells), and MCF7 (breast cancer cells) cells after incubation with the PEG-modified BPQDs at different concentrations (20, 50, 100, 150, and 200 ppm) for 48 hours. No cytotoxicity could be observed for the four types of cells even at a high concentration of 200 ppm, which is much higher

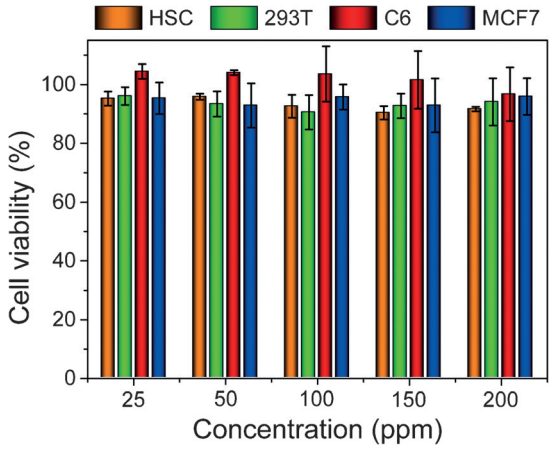

Figure 3. Relative viabilities of HSC, 293T, C6, and MCF7 cells after incubation with various concentrations (20, 50, 100, 150, and 200 ppm) of PEG-modified BPQDs for 48 h.

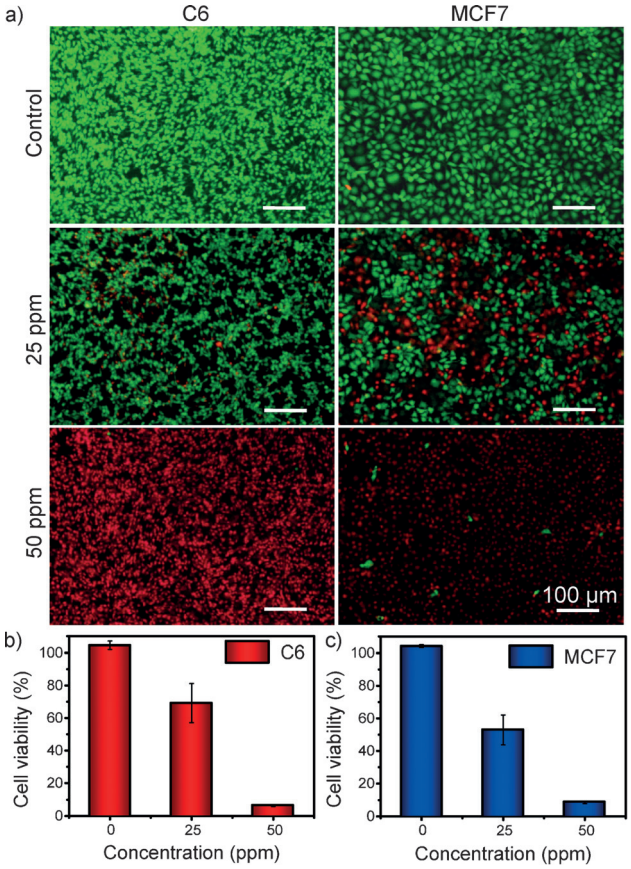

Figure 4. Comparison of the photothermal destruction of C6 and MCF7 cancer cells upon addition of BPQDs (0, 25, or 50 ppm) and irradiation with an 808 nm laser at 1.0 $W cm^{-2}$ for 10 min. a) Fluorescence images of cells stained with calcein AM (live cells, green fluorescence) and PI (dead cells, red fluorescence). b) Relative viabilities of C6 cells after the various treatments. c) Relative viabilities of MCF7 cells after the various treatments. Error bars are based on the standard deviations (SDs) of six parallel samples.

than that used in the following photothermal experiments, suggesting good biocompatibility and suitability for biomedical applications.

The photothermal effect of the BPQDs in cancer cells was then investigated (Figure 4). C6 and MCF7 cancer cells were incubated with the BPQDs for fours hours, and the cells were illuminated with an NIR laser (808 nm, 1.0 $W cm^{-2}$) for 10 min. The live/dead cells were differentiated by calcein AM (live cells, green fluorescence) and propidium iodide (PI; dead cells, red fluorescence) co-staining after the PTT treatment (Figure 4a). A BPQD-dose-dependent PTT effect was observed for both the C6 and MCF7 cells. Almost all of the cells were killed after incubating with only 50 ppm of the PEG-modified BPQDs and exposure to the NIR laser. In contrast, exposure of the cells to the NIR laser in the absence of the BPQDs did not compromise cell viability. Similar results were also obtained by the standard MTT assay (Figure 4b,c). Furthermore, the BPQDs showed no dark toxicity to these cells at concentrations between 20 and 200 ppm (see Figure 3). These results clearly demonstrate the good PPT efficiency of the BPQDs in promoting cancer cell death. It should be noted that by using only 50 ppm of the BPQDs, the threshold of photothermal cell destruction using an 808 nm laser was 1.0 $W cm^{-2}$ for 10 min. These conditions are more moderate than those adopted for in vitro photothermal cell destruction with Au nanoshells (35 $W cm^{-2}$, 7 min)[29] and copper selenide nanocrystals (30 $W cm^{-2}$, 5 min).[13] The excellent PPT efficiency of the BPQDs is probably due to their ultrasmall size, facilitating their cellular internalization into cancer cells.

In summary, a controllable liquid exfoliation method for the synthesis of black phosphorus quantum dots has been described, and their effectiveness as NIR photothermal agents has been assessed. With a lateral size of approximately 2.6 nm and a thickness of about 1.5 nm, the ultrasmall BPQDs exhibited an excellent NIR photothermal performance with a large extinction coefficient of 14.8 $L g^{-1} cm^{-1}$ at 808 nm, a photothermal conversion efficiency of 28.4%, as well as good photostability. After PEG conjugation, the BPQDs showed enhanced stability in physiological medium, and there was no observable toxicity to different types of cells. NIR photoexcitation of the BPQDs in the presence of C6 and MCF7 cancer cells led to significant cell death, suggesting that the nanoparticles have large potential in PTT applications. Owing to their ultrasmall size, the BPQDs have a long blood circulation time, enabling the attachment of additional non-immunogenic or cellular targeting molecules for targeted photothermal cancer therapy.

Acknowledgements

This work was supported by the NSFC (51372175, 61222505, 61435010), the Science and Technology Key Project of Shenzhen (JCYJ20140417113430608), the Shenzhen Key Laboratory for Molecular Biology of Neural Development (ZDSY20120617112838879), the Hong Kong Research Grants Council (RGC) General Research Funds (GRF; 112212), and the City University of Hong Kong Strategic Research Grant (SRG; 7004188).

Keywords: black phosphorus · nanocrystals · photothermal agents · photothermal therapy · quantum dots

How to cite: *Angew. Chem. Int. Ed.* **2015**, *54*, 11526–11530
Angew. Chem. **2015**, *127*, 11688–11692

[1] R. Weissleder, *Nat. Biotechnol.* **2001**, *19*, 316.
[2] a) L. R. Hirsch, R. J. Stafford, J. A. Bankson, S. R. Sershen, B. Rivera, R. E. Price, J. D. Hazle, N. J. Halas, J. L. West, *Proc. Natl. Acad. Sci. USA* **2003**, *100*, 13549; b) X. H. Huang, I. H. El-Sayed, W. Qian, M. A. El-Sayed, *J. Am. Chem. Soc.* **2006**, *128*, 2115; c) T. S. Hauck, T. L. Jennings, T. Yatsenko, J. C. Kumaradas, W. C. W. Chan, *Adv. Mater.* **2008**, *20*, 3832.
[3] a) K. Dong, Z. Liu, Z. Li, J. Ren, X. Qu, *Adv. Mater.* **2013**, *25*, 4452; b) W. Y. Yin, L. Yan, J. Yu, G. Tian, L. J. Zhou, X. P. Zheng, X. Zhang, Y. Yong, J. Li, Z. J. Gu, Y. L. Zhao, *ACS Nano* **2014**, *8*, 6922.
[4] K. C. Hribar, Y. S. Choi, M. Ondeck, A. J. Engler, S. C. Chen, *Adv. Funct. Mater.* **2014**, *24*, 4922.
[5] L. Cheng, C. Wang, L. Feng, K. Yang, Z. Liu, *Chem. Rev.* **2014**, *114*, 10869.
[6] a) L. Cheng, J. J. Liu, X. Gu, H. Gong, X. Z. Shi, T. Liu, C. Wang, X. Y. Wang, G. Liu, H. Y. Xing, W. B. Bu, B. Q. Sun, Z. Liu, *Adv. Mater.* **2014**, *26*, 1886; b) W. Lu, C. Xiong, G. Zhang, Q. Huang, R. Zhang, J. Z. Zhang, C. Li, *Clin. Cancer Res.* **2009**, *15*, 876.
[7] a) Y. Pan, S. Neuss, A. Leifert, M. Fischler, F. Wen, U. Simon, G. Schmid, W. Brandau, W. Jahnen-Dechent, *Small* **2007**, *3*, 1941; b) H. Soo Choi, W. Liu, P. Misra, E. Tanaka, J. P. Zimmer, B. I. Ipe, M. G. Bawendi, J. V. Frangioni, *Nat. Biotechnol.* **2007**, *25*, 1165; c) M. Longmire, P. L. Choyke, H. Kobayashi, *Nanomedicine* **2008**, *3*, 703; d) W. Jiang, B. Y. Kim, J. T. Rutka, W. C. Chan, *Nat. Nanotechnol.* **2008**, *3*, 145.
[8] H. Liu, D. Chen, L. Li, T. Liu, L. Tan, X. Wu, F. Tang, *Angew. Chem. Int. Ed.* **2011**, *50*, 891; *Angew. Chem.* **2011**, *123*, 921.
[9] M. S. Yavuz, Y. Cheng, J. Chen, C. M. Cobley, Q. Zhang, M. Rycenga, J. Xie, C. Kim, K. H. Song, A. G. Schwartz, L. V. Wang, Y. Xia, *Nat. Mater.* **2009**, *8*, 935.
[10] S. H. Tang, X. Q. Huang, N. F. Zheng, *Chem. Commun.* **2011**, *47*, 3948.
[11] J. T. Robinson, S. M. Tabakman, Y. Liang, H. Wang, H. S. Casalongue, D. Vinh, H. Dai, *J. Am. Chem. Soc.* **2011**, *133*, 6825.
[12] N. W. Shi Kam, M. O'Connell, J. A. Wisdom, H. J. Dai, *Proc. Natl. Acad. Sci. USA* **2005**, *102*, 11600.
[13] C. M. Hessel, V. P. Pattani, M. Rasch, M. G. Panthani, B. Koo, J. W. Tunnell, B. A. Korgel, *Nano Lett.* **2011**, *11*, 2560.
[14] A. M. Gobin, M. H. Lee, N. J. Halas, W. D. James, R. A. Drezek, J. L. West, *Nano Lett.* **2007**, *7*, 1929.
[15] B. Tian, C. Wang, S. Zhang, L. Z. Feng, Z. Liu, *ACS Nano* **2011**, *5*, 7000.
[16] X. Huang, S. Neretina, M. A. El-Sayed, *Adv. Mater.* **2009**, *21*, 4880.
[17] J. Y. Chen, C. Glaus, R. Laforest, Q. Zhang, M. X. Yang, M. Gidding, M. J. Welch, Y. N. Xia, *Small* **2010**, *6*, 811.
[18] K. Yang, S. Zhang, G. Zhang, X. Sun, S. T. Lee, Z. Liu, *Nano Lett.* **2010**, *10*, 3318.
[19] S. S. Chou, B. Kaehr, J. Kim, B. M. Foley, M. De, P. E. Hopkins, J. Huang, C. J. Brinker, V. P. Dravid, *Angew. Chem. Int. Ed.* **2013**, *52*, 4160; *Angew. Chem.* **2013**, *125*, 4254.
[20] M. Li, X. J. Yang, J. S. Ren, K. G. Qu, X. G. Qu, *Adv. Mater.* **2012**, *24*, 1722.
[21] B. Li, K. C. Ye, Y. X. Zhang, J. B. Qin, R. J. Zou, K. B. Xu, X. J. Huang, Z. Y. Xiao, W. J. Zhang, X. W. Lu, J. Q. Hu, *Adv. Mater.* **2015**, *27*, 1339.
[22] H. Liu, Y. Du, Y. Deng, P. D. Ye, *Chem. Soc. Rev.* **2015**, *44*, 2732.
[23] a) J. R. Brent, N. Savjani, E. A. Lewis, S. J. Haigh, D. J. Lewis, P. O'Brien, *Chem. Commun.* **2014**, *50*, 13338; b) J. Kang, J. D. Wood, S. A. Wells, J. H. Lee, X. Liu, K. S. Chen, M. C. Hersam, *ACS Nano* **2015**, *9*, 3596; c) P. Yasaei, B. Kumar, T. Foroozan, C. Wang, M. Asadi, D. Tuschel, J. E. Indacochea, R. F. Klie, A. Salehi-Khojin, *Adv. Mater.* **2015**, *27*, 1887; d) X. Zhang, H. Xie, Z. Liu, C. Tan, Z. Luo, H. Li, J. Lin, L. Sun, W. Chen, Z. Xu, L. Xie, W. Huang, H. Zhang, *Angew. Chem. Int. Ed.* **2015**, *54*, 3653; *Angew. Chem.* **2015**, *127*, 3724.
[24] a) F. N. Xia, H. Wang, Y. C. Jia, *Nat. Commun.* **2014**, *5*, 4458; b) J. Qiao, X. Kong, Z. X. Hu, F. Yang, W. Ji, *Nat. Commun.* **2014**, *5*, 4475; c) J. D. Wood, S. A. Wells, D. Jariwala, K. S. Chen, E. Cho, V. K. Sangwan, X. Liu, L. J. Lauhon, T. J. Marks, M. C. Hersam, *Nano Lett.* **2014**, *14*, 6964; d) M. Buscema, D. J. Groenendijk, S. I. Blanter, G. A. Steele, H. S. J. van der Zant, A. Castellanos-Gomez, *Nano Lett.* **2014**, *14*, 3347; e) H. Wang, X. Wang, F. Xia, L. Wang, H. Jiang, Q. Xia, M. L. Chin, M. Dubey, S. J. Han, *Nano Lett.* **2014**, *14*, 6424; f) X. Wang, A. M. Jones, K. L. Seyler, V. Tran, Y. Jia, H. Zhao, H. Wang, L. Yang, X. Xu, F. Xia, *Nat. Nanotechnol.* **2015**, *10*, 517.
[25] H. Liu, A. T. Neal, Z. Zhu, Z. Luo, X. Xu, D. Tomanek, P. D. Ye, *ACS Nano* **2014**, *8*, 4033.
[26] a) B. Thierry, L. Zimmer, S. McNiven, K. Finnie, C. Barbe, H. J. Griesser, *Langmuir* **2008**, *24*, 8143; b) S. Liufu, H. Xiao, Y. P. Li, *Powder Technol.* **2004**, *145*, 20.
[27] D. K. Roper, W. Ahn, M. Hoepfner, *J. Phys. Chem. C* **2007**, *111*, 3636.
[28] B. Wang, J. H. Wang, Q. Liu, H. Huang, M. Chen, K. Li, C. Li, X. F. Yu, P. K. Chu, *Biomaterials* **2014**, *35*, 1954.
[29] M. P. Melancon, W. Lu, Z. Yang, R. Zhang, Z. Cheng, A. M. Elliot, J. Stafford, T. Olson, J. Z. Zhang, C. Li, *Mol. Cancer Ther.* **2008**, *7*, 1730.

Received: July 4, 2015
Published online: August 21, 2015

